Available online at www.sciencedirect.com
ScienceDirect
Powder Technology 181 (2008) 121–129
POWDER TECHNOLOGY
www.elsevier.com/locate/powtec

Numerical and experimental investigation of capping mechanisms during pharmaceutical tablet compaction

C.-Y. Wu [a,*], B.C. Hancock [b], A. Mills [c], A.C. Bentham [c], S.M. Best [a], J.A. Elliott [a]

[a] *Pfizer Institute for Pharmaceutical Materials Science, Department of Materials Science and Metallurgy, University of Cambridge, Pembroke Street, Cambridge, CB2 3QZ, UK*
[b] *Pfizer Global Research and Development, Groton, CT 06340, USA*
[c] *Pfizer Global Research and Development, Sandwich, Kent, CT13 9NJ, UK*

Available online 14 December 2006

Abstract

Capping is a common problem in the pharmaceutical tabletting process in which catastrophic failure of the powder compact can occur. It is of great interest to the pharmaceutical industry to understand the fundamental reasons why capping occurs and how it can be avoided. Recently, a combined numerical and experimental study on pharmaceutical powder compaction revealed that cone capping, which is a typical failure mechanism during the production of flat-faced cylindrical tablets using powders of low tensile strength, is due to the formation of a narrow band with localised, intensive shear stresses running from the top edge towards the bottom centre of the tablet [C.Y. Wu, O. Ruddy, A.C. Bentham, B.C. Hancock, S.M. Best, J.A. Elliott, Modelling the mechanical behaviour of pharmaceutical powders during compaction, *Powder Technology*, 152 (2005)107–117.]. In this paper, the results of further studies are reported in an attempt to explore possible methods to alleviate the propensity for tablets to cap. These methods have been systematically investigated using finite element methods (FEM), and include using lubrication to reduce the die-wall friction, employing different tooling kinematics (speeds and compression profiles), making tablets with different thicknesses, and making convex tablets using punches with curved surfaces. It has been found that none of these methods could avoid the development of intensive shear bands during unloading, which implies that capping cannot necessarily be avoided using these methods. In addition, physical experiments using a compaction simulator have also been carried out, in particular, for making convex tablets with different curvatures. The tablets produced were examined using X-ray microtomography (XMT), from which the failure patterns were identified and found to be in very good agreement with the numerical analysis. The combination of experimental and numerical studies has demonstrated that: (i) capping takes place during the decompression (unloading) phase, and (ii) the intensive shear bands formed during decompression are responsible for the occurrence of capping.

Keywords: Failure mechanisms; Powder compaction; Tablet; Finite element modelling; Capping; X-ray tomography

1. Introduction

The tablet is a very common and popular dosage form for drug delivery in the pharmaceutical industry. It is generally manufactured by compacting dry powder blends. The manufacturing process is similar to those used to make green compacts in powder metallurgy and in the ceramic industry and can be divided into three distinct stages: (i) die filling, (ii) compaction, and (iii) ejection. During die filling, the powder blends are deposited into the die cavity under gravity from a feed shoe that runs over the die opening [2–4]. The powder is then compressed inside a die by two punches during compaction, where individual powder particles experience intensive deformation and start to bond together through van der Waals forces, mechanical interlocking and formation of solid bridges [5]. Finally, the compacted powder is ejected from the die in the form of a tablet. The properties of the tablet depend significantly upon the powder behaviour during all the three stages of the process [6]. Therefore, an understanding of the mechanical behaviour of the powder during each stage is vital for successful formulation processing.

Among these stages, compaction is the most crucial phase because the powder bed experiences intensive densification and high stresses are developed as the two punches move towards each other until the tablet press reaches its specified state (*i.e.* maximum compression pressure or minimum punch separation). Thereafter, decompression takes place once the two punches start

* Corresponding author.
E-mail address: C.Y.Wu@bham.ac.uk (C.-Y. Wu).

0032-5910/$ - see front matter © 2007 Elsevier B.V. All rights reserved.
doi:10.1016/j.powtec.2006.12.017

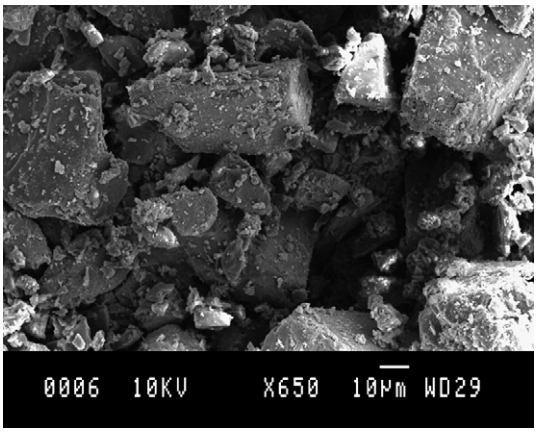

Fig. 1. SEM image of the lactose powder considered in this study, showing the particle morphology.

to move away from each other. During this stage, the compaction pressure drops quickly as the distance between two punches increases, and elastic strain accumulated during compression recovers. This is accompanied by an increase in the volume of the powder bed and a consequent decrease in the relative density.

It is generally thought that the elastic recovery rate during decompression is one of the primary factors responsible for the occurrence of defects, such as cracks and fracture of powder compacts, as faster elastic recovery is more likely to cause the failure [7–9]. Some also anticipate that the failure of tablets during tabletting is due to the entrapment of air, which prevents strong bonding from being established during the compaction phase [10]. Both theories appear reasonable, however very little direct evidence for either hypothesis has been reported in the literature so far. Based upon a combination of numerical and experimental investigation, a study by the present authors recently found that the tablet failure, in particular capping, is associated with an intensive shear band formed during the decompression stage [1]. It is hence of interest to explore the methods which can alleviate the capping tendencies.

The aim of this paper is therefore to present some further studies on capping mechanisms and a systematic investigation of possible methods to alleviate the propensity for capping. Again, a combined investigation including experimental and numerical analyses has been carried out. For the numerical analysis, the material properties for lactose reported in Ref. [1], which were extracted from uniaxial compaction experiments using a compaction simulator with an instrumented die, were used in constitutive models for the FE simulations. Various possible approaches to alleviate the capping tendency are then considered. These included using concave-shaped punches to make convex tablets, employing different tooling kinematics (varying both speeds and compression profiles), reducing the maximum compression pressure and varying the die-wall friction. An emphasis is placed upon whether there was an intensive shear band formed during decompression, as this is believed to be responsible for the occurrence of capping. The experimental study has two purposes: (i) to characterise the material properties of the powder considered and to determine realistic material properties for using in the numerical analysis, and (ii) to visualise the failure patterns of tablets, for which X-ray microtomography (XMT) is employed.

2. Experimental procedures

Lactose powder, which is widely used in the pharmaceutical industry as a diluent, was considered in this study. Fig. 1 shows a SEM image of lactose powder, illustrating the morphology of the powder particles. The lactose powder had a true density of 1548 kg m^{-3}. Uniaxial compaction tests were conducted using an instrumented hydraulic press (compaction simulator, ESH, Brierley Hill, West Midlands, UK). Two types of experiments were carried out: (i) calibration tests with an instrumented die, in which a cylindrical die of 8 mm in diameter with radial stress sensors was used together with flat-faced punches to compress the powders, and (ii) visualisation of failure patterns using XMT, in which standard tooling with various punch surfaces were chosen to make both flat-faced and convex tablets that were then examined using XMT. For both types of experiments, the powder was compressed using a single-ended compaction profile, in which only the upper punch was moving downwards

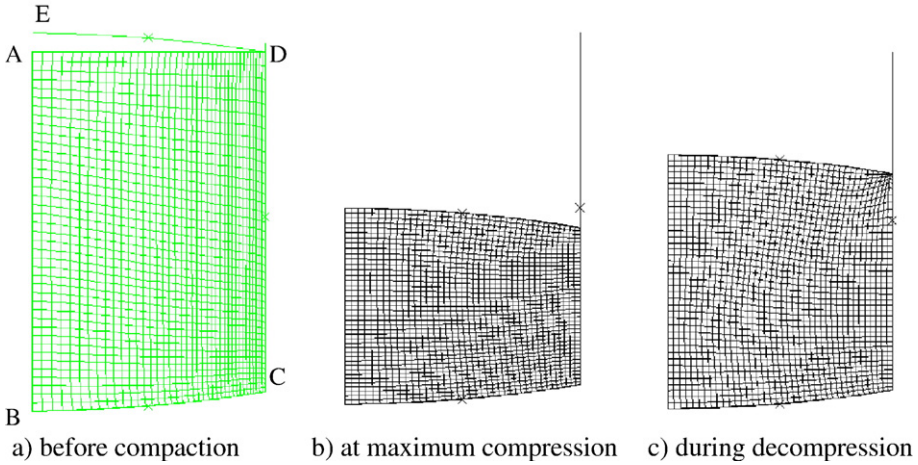

Fig. 2. FE meshes for modelling the compaction of shallow convex tablets.

Fig. 3. A photography of broken flat-faced cylindrical tablets [1] showing the cone capping failure pattern.

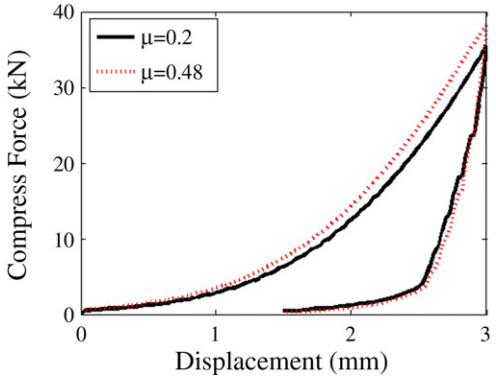

Fig. 5. The force–displacement curves during the compactions with different die-wall frictions.

to compress the powder, with the lower punch held stationary during the whole compaction process. A "V" shaped compaction profile was employed and the compacted tablets were ejected immediately after the top punch was withdrawn to its starting position.

2.1. Calibration tests with an instrumented die

In these experiments, the powder was manually poured into a die cavity of 13 mm in depth until a small heap of powder developed above the top surface of the die. The excess powder above the top surface of the die was scraped off with a blade so that the die was fully occupied by loosely packed powder. The compression (loading) and decompression (unloading) speeds were set to 3 mm s^{-1}. During the tests, the axial forces on the upper and lower punches were recorded with load cells of 50 kN capacity. The displacement of the upper punch was measured with a linear variable differential transformer (LVDT) displacement transducer. The radial stress was also measured with a pressure sensor of 200 MPa capacity. The axial stress, axial strain and radial stress were then determined. Knowing the axial stress–strain relation and the relation between deviatoric stress and mean stress, the material properties can then be determined in line with Drucker–Prager Cap (DPC) model used in the FE analysis. A more detailed description of the methods to extract the material properties can be found in Ref. [1]. The materials properties determined for the lactose powder considered are as follows: Young's modulus E=3.57 GPa, Poisson's ratio v=0.12, cohesion d=0.91 kPa and the friction angle β=41.02°. By setting the geometry parameters (α, R) to α=0.03 and R=0.6, the hardening mechanism in the DPC model, which is generally referred to as the evolution of the cap surface, can be defined as a variation of the hydrostatic yield stress p_b with the volumetric plastic strain ε_{vol}^{in}. A least-squares best fit to the experimental data gave the following expression:

$$p_b = 8.12 \times 10^{-4} e^{9.05\varepsilon_{vol}^{in}}. \quad (1)$$

The die-wall friction was determined according to the Janssen–Walker theory [1,11,12]. The effect of lubrication on the die-wall friction was also investigated by using either a lubricated die, or a clean die without lubrication. For the tests with lubricated die, a 1% concentration of magnesium stearate in ethanol was used, which was applied onto the die wall to form a thin layer of lubricant. For both cases, a constant die-wall coefficient of friction was assumed in the simulations reported in the next section, which was obtained by averaging the experimental data over compaction pressures between 40 MPa and 100 MPa. For the lubricated die, the die-wall coefficient of friction of μ=0.20 was used, while for unlubricated die μ=0.48.

2.2. Visualisation of failure patterns using XMT

X-ray computed tomography is a non-destructive technique that can be used to visualise the internal structure of materials [13–15]. This technique uses an array of detectors to measure the attenuation of two-dimensional cone beams of X-rays that penetrate the sample. The two-dimensional (2D) radiographic

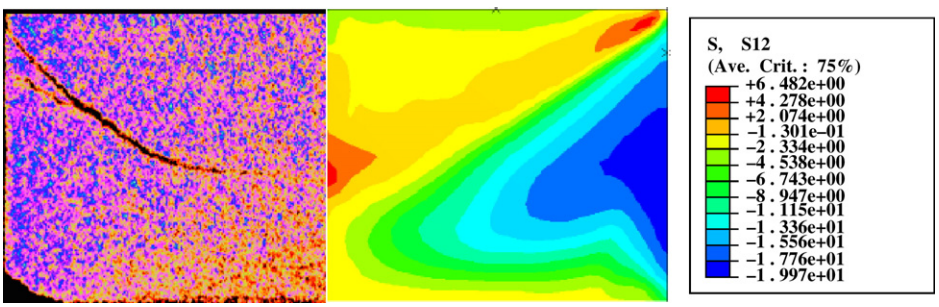

Fig. 4. X-ray tomographic image showing the pattern of cracking (left) and shear stress distribution (right) showing that there is a shear band from top edge towards the mid-centre (μ=0.48).

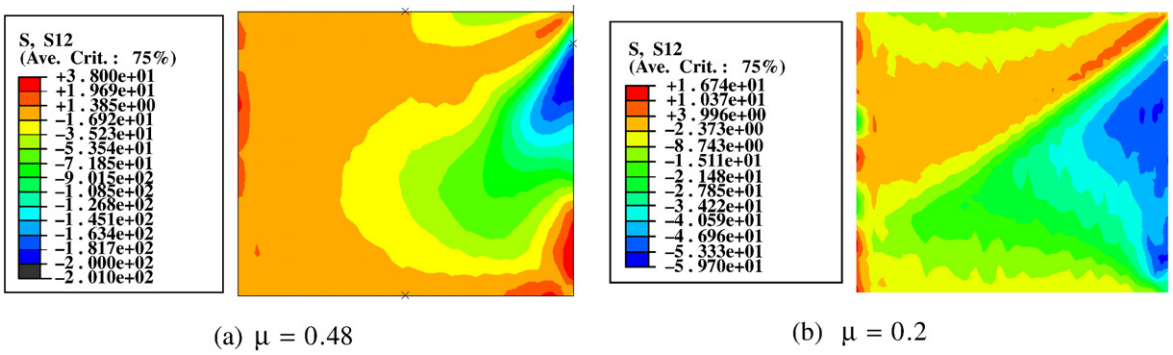

(a) μ = 0.48 (b) μ = 0.2

Fig. 6. The shear stress distribution during decompression for the compactions with different die-wall frictions.

projections of a sample are then used to reconstruct a three-dimensional (3D) image of the X-ray attenuation coefficient of the material. The degree of X-ray attenuation depends on the atomic number and mass density of the samples. A higher attenuation of the X-rays is generally obtained for materials with higher density and larger atomic number. Therefore, X-ray tomography can distinguish between the different phases and/or components in a material in a non-destructive manner. Recent advances in X-ray tomography have made it possible to visualise the internal structures of certain materials with a spatial resolution of several micrometres, even down to the sub-micrometre level [15]. It has hence been widely used in the visualisation of cracks in a number of different materials [16–21]. In this study, we have used a desktop high-resolution micro-CT system (Skyscan 1072, SkyScan, Aartselaar, Belgium) with a spatial resolution of 5 μm to visualise the failure patterns of pharmaceutical tablets.

The flat-faced round tablets produced from the calibration experiments were first examined using XMT. The failure patterns of these tablets were observed and have been previously presented in Ref. [1]. In addition, as an attempt to alleviate the propensity for tablet to cap, convex round tablets of different surface curvatures were also produced using the compaction simulator with standard tooling. All the tablets had a diameter of 8 mm but two different surface curvatures were considered: (i) shallow convex tablets, for which the radius of the surface curvature was 13.5 mm and the punch depth was 0.58 mm, and (ii) standard convex tablets, for which the radius of the surface curvature was 9.5 mm and the punch depth was 0.85 mm. During these tests, a slightly lower compaction speed than that was used in calibration tests was chosen (0.3 mm s^{-1}) in order to allow any entrapped air enough time to escape during the compaction. The tablets were also examined using XMT, and the failure patterns were observed and will be presented in this paper.

3. Numerical modelling

Finite element methods (FEM) are now a well-established method for modelling the deformation of powders in various industries, such as compaction of metallic and ceramic powders in powder metallurgy and ceramic industries [22–27], and analysing pharmaceutical powder compaction [1,11,28]. The material properties and die-wall friction, calibrated from experiments with the instrumented die as given in Section 2.1, were input into a commercial package, ABAQUS [29], in which the Drucker–Prager Cap (DPC) model was implemented.

Since the compaction of cylindrical tablets is an axisymmetric case, it can be analysed using a two-dimensional finite element model. Fig. 2 shows the typical FE meshes for modelling the compaction of convex tablets, where Fig. 2a shows the meshes before compaction, Fig. 2b shows the mesh at the point of maximum compression and Fig. 2c shows the meshes during decompression. Due to the symmetry, only half of the vertical cross-section needs to be discretised, and this was done with four node axisymmetric continuum elements. The die wall and upper punches were modelled as rigid bodies. The interaction between the powder, die wall and upper punch was

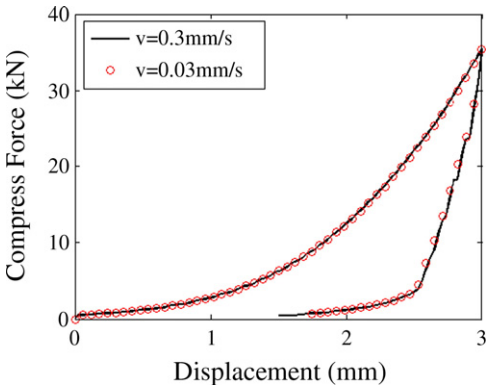

Fig. 7. The force–displacement curves during the compactions at different speeds (μ=0.2).

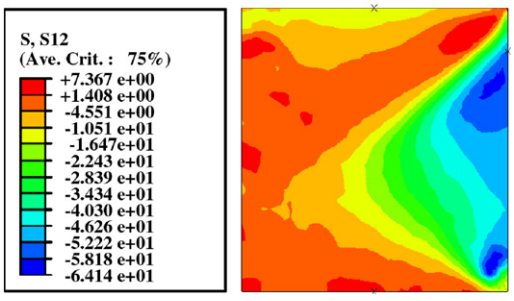

Fig. 8. The shear stress distribution during decompression for the compaction at a speed of 0.03 mm s^{-1} (μ=0.2).

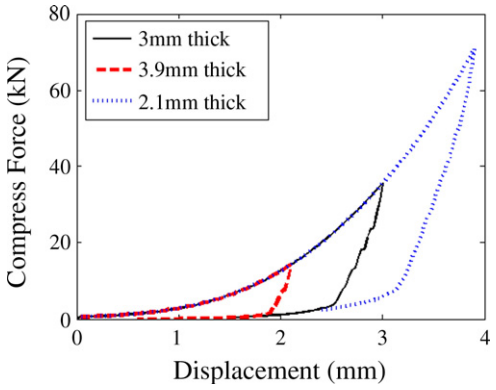

Fig. 9. The force–displacement curves during the compactions with various minimum thicknesses (μ=0.2).

modelled by master–slave contacts with finite sliding. The friction in the contacts was set to the values determined from experiments. The nodes on the symmetry axis (AB) were restricted to move in horizontal direction, and the nodes at top and bottom boundaries AD and BC are only allowed to move along the specified curve. Both upper and lower punches, modelled as rigid walls (BC and DE), can move vertically with a compression speed as specified in the compaction profile.

The results from the numerical modelling will be given in the next section. We first consider the simplest tablet shape — flat face round tablets, as analysed in Ref. [1], but employing different compaction conditions. These compaction conditions include using lubrication to reduce the die-wall friction, reducing the compaction speed, making a thinner or thicker tablet, and using different compaction profile (*i.e.* using double-ended compaction instead of single-ended compaction). We then proceed to describe simulations using punches with curved surfaces to make convex tablets, for which two different punch surfaces curvatures widely used in pharmaceutical industry were chosen.

4. Results

The numerical and experimental investigations reported in Ref. [1] reveal that cone capping is a common phenomenon in making flat-faced round tablets with lactose. A photograph of some capped tablets described in Ref. [1] is given in Fig. 3, which shows that the tablets have broken into two halves, with the top half being a cone shape. We have examined some of the tablets, that were not visibly broken, using XMT, and found that there are cracks inside the tablet which form a cone-shaped failure surface [1], as illustrated in Fig. 4 (left-hand side). It is clear that cracks develop from the top edge towards the mid-centre of the tablet. On the right-hand side of Fig. 4, the shear stress distribution during decompression obtained from finite element analysis is superimposed. It is clear that there is a shear band running from the top edge towards the mid-centre. Comparing the X-ray tomographic image with the shear stress distribution indicates that the locus of the shear band is very similar to the pattern of cracks and capping shown in Fig. 3. It is of interest in tablet formulation to explore the possible approaches to avoid the occurrence of capping. In the following sub-sections, some systematic analysis using finite element methods is presented. As the shear band formed during decompression is responsible for the occurrence of capping, we shall concentrate on patterns of the shear stress distribution during decompression in the following discussions.

4.1. Effect of die-wall friction

We consider a case where a lactose powder bed of 8 mm in diameter has an initial height of 6 mm and is compressed into a minimum thickness of 3 mm following a single-ended compaction (SEC) profile. Both the compression and decompression speeds were set to be 0.3 mm s^{-1}. The material properties of lactose given in Section 2 were used in the FE analysis. Die-wall coefficients of friction obtained from experiments with both lubricated (μ=0.20) and unlubricated dies (μ=0.48) were considered. Fig. 5 shows the force–displacement curves during compactions with the two different coefficients of die-wall friction. It can be seen that the overall patterns of force–displacement curves with different die-wall frictions are similar, and are also consistent with the pattern reported by Zahlan et al. [30]. Furthermore, as expected, the forces evolved during compression are slightly higher when a higher die-wall friction was used. There was no significant difference in the force–displacement curves during decompression for the different die-wall frictions.

The corresponding shear stress distributions at the early stage of decompression are presented in Fig. 6. Note that the left-hand sides of both Fig. 6a and b correspond to the central axis of the

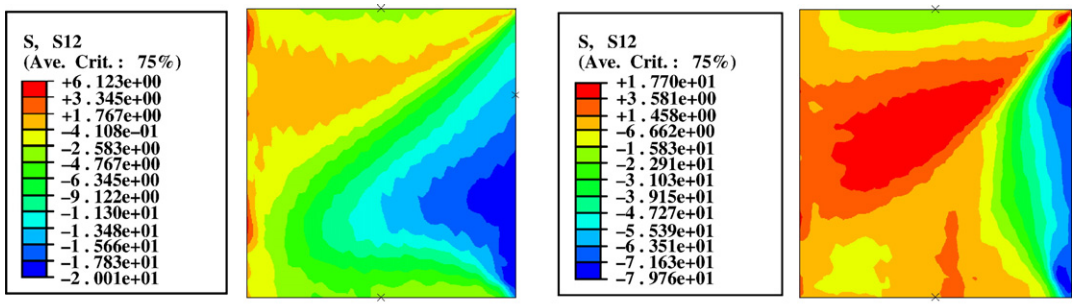

(a) H_{min} = 3.9mm (b) H_{min} = 2.1mm

Fig. 10. The shear stress distribution during decompression for the compactions with different minimum thicknesses (μ=0.2).

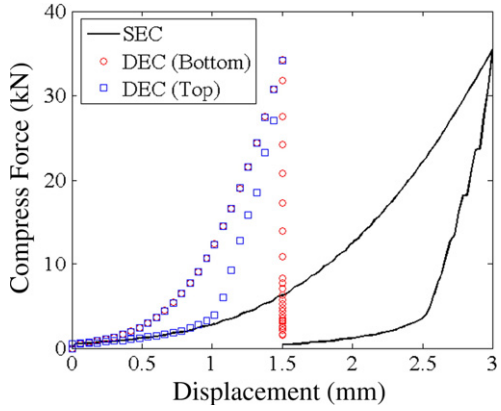

Fig. 11. The force–displacement curves during the compactions with different profiles (μ=0.2).

tablet, and the right-hand sides to the edge of the tablet. It is clear that for the compactions with both high and low die-wall frictions there are intensive shear bands running from the top edge towards the mid-centre of the tablets, and that the patterns are similar to that shown on the right-hand side of Fig. 4. This implies that it is possible for capping to be induced for both cases. This was demonstrated with our experimental observations presented in Ref. [1] that capped tablets were still produced even if the lubrication was applied on the die wall. Therefore, only the lower die-wall friction will be considered in the following sections.

4.2. Effect of compaction speed

Decreasing the compaction speed will reduce the rate of stress relaxation during decompression, and thus it could conceivably be beneficial for alleviating the propensity for the tablet to cap. Further to the case shown in Fig. 6b, where the compression speed was set to 0.3 mm s^{-1}, we reduced the compaction speed by one order of magnitude to 0.03 mm s^{-1}. Fig. 7 shows the force–displacement curves during compaction at these two speeds. It is interesting to see that the force–displacement curves for two different compression speeds are almost indistinguishable. The shear stress distribution at the early stage of decompression at a speed of 0.03 mm s^{-1} is shown in Fig. 8. It is clear that the pattern is similar to that shown in Fig. 6b for a compaction speed of 0.3 mm s^{-1}. A band

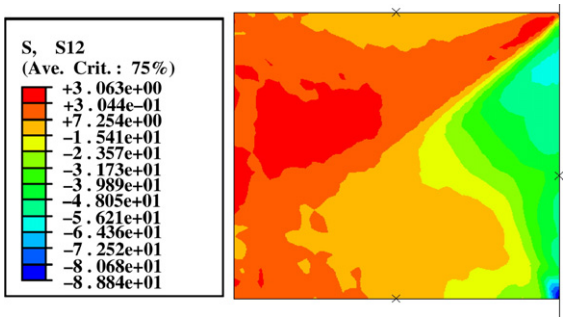

Fig. 12. The shear stress distribution during decompression for the compaction with double-ended compaction profile (μ=0.2).

Table 1
Parameters for simulating the compaction of flat-faced and convex tablets

Tablet shape	Initial powder height (mm)	Powder height at maximum compression (mm)	Punch travel distance (mm)
Flat-faced	6	3	3
Shallow convex	5.83	2.67	3.16
Standard convex	5.56	2.13	3.43

with intensive shear stress is also developed for the compaction at very low speeds, which indicates that capping can still be induced.

4.3. Effect of tablet thickness

Tablets with different thicknesses can be produced by compressing the powder bed to different minimum heights (*i.e.*, with different maximum compression pressure), which will result in different degrees of deformation of the powder bed. Fig. 9 shows the force–displacement curves for the compaction of a powder bed with an initial height of 6 mm down to minimum thicknesses of 3.9 mm (thickest), 3 mm and 2.1 mm (thinnest), as measured at the point of maximum compression pressure. It is clear that the loading curves follow the same overall trajectory, but that the maximum compression force increases sharply as the minimum thickness of the tablet decreases. The shear stress distributions during decompression for making the thickest and thinnest tablets are shown in Fig. 10. In comparison to Fig. 6b, it is clear that for all three cases considered, the shear bands are still developed during the compaction of tablets with different thicknesses. This implies again that capping is still possible for manufacturing tablets of different thicknesses.

4.4. Effect of compaction profile

Double-ended compaction (DEC) is a common practice in pharmaceutical tablet production, in which the powder bed is compressed by both top and bottom punches as they move towards each other [31]. Double-ended compaction of a powder bed with an initial height of 6 mm down to minimum thickness of 3 mm at maximum compression was also

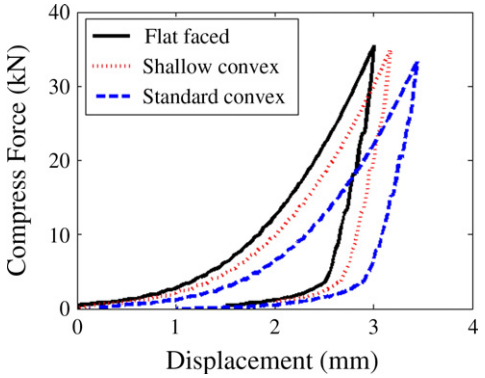

Fig. 13. The force–displacement curves for the compactions with punches of various surface curvatures (μ=0.2).

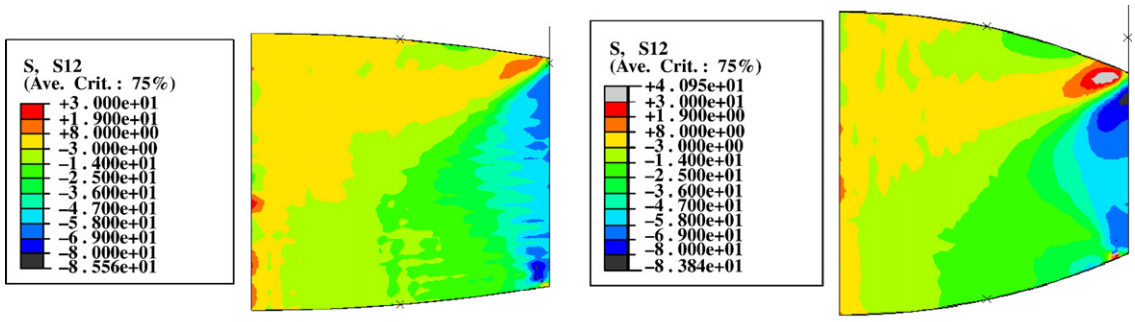

(a) shallow convex (b) standard convex

Fig. 14. The shear stress distribution during decompression for the compaction of convex tablets with different surface curvatures (μ=0.2).

modelled using FEA. Both the top and bottom punches were moved at a speed of 0.3 mm s^{-1} during the compression. During the decompression, the top punch was released at the same speed, but the bottom punch remained stationary. The force–displacement curves for both DEC and SEC profiles are given in Fig. 11. It can be seen that during compression phase of DEC, the force–displacement curves obtained from both the top and bottom punches are identical. In addition, it is interesting to find that the maximum compression forces are equal for both SEC and DEC. Fig. 12 shows the shear stress distribution during decompression of making a tablet with DEC profile. It can be seen that there is again an intensive shear band as shown for SEC in Figs. 6b and 4. This implies that cone capping still can happen even if the powder is compressed using a DEC profile.

4.5. Effect of surface curvature

Another option that might be used as an attempt to avoid the occurrence of capping is to make convex tablets using punches with concave surfaces. FE simulations of the compaction of convex tablets with different surface curvatures using a SEC profile were therefore performed. Two types of convex tablets were considered: shallow convex and standard convex tablets (with surface curvatures and punch depths as defined in Section 2.2). For the purpose of achieved a better comparison to the flat-faced tablets shown in Fig. 6b, the diameter of these convex tablets were also set to be 8 mm. In addition, the initial volume of the powder bed and the volume at maximum compression for making convex tablets and flat-faced tablets were set to be identical. This means that, among the three cases, the initial heights of powder beds were different and the total travel distances of the top punch were also different. These parameters are given in Table 1, and the compaction speed was set to 0.3 mm s^{-1}.

Fig. 13 shows the variations of the (axial) compression force with the displacement of the top punches for making flat-faced, shallow convex and standard convex tablets in SEC mode. It can be seen that the overall pattern of force–displacement curves for the various punch surfaces are rather similar for low displacements. However, the force–displacement curves shift towards the right-hand side with a slight decrease in the maximum compression force as the curvature of the punch surface increases (*i.e.* as the radius of the surface curvature decreases). The shear stress distributions during decompression for compacting convex tablets are given in Fig. 14. It can be seen that there are also intensive shear bands developed for both cases. Furthermore, the shear band developed for convex tablets appear to be less oblique than that for flat-faced tablets (Fig. 6b), which implies that the failure surfaces for capping become less oblique. This has been confirmed by our experimental observations, as shown in Figs.15 and 16. Fig. 15 shows photographs of shallow convex (Fig. 15a) and standard convex tablets (Fig. 15b) which have visible failures (chipping and capping).

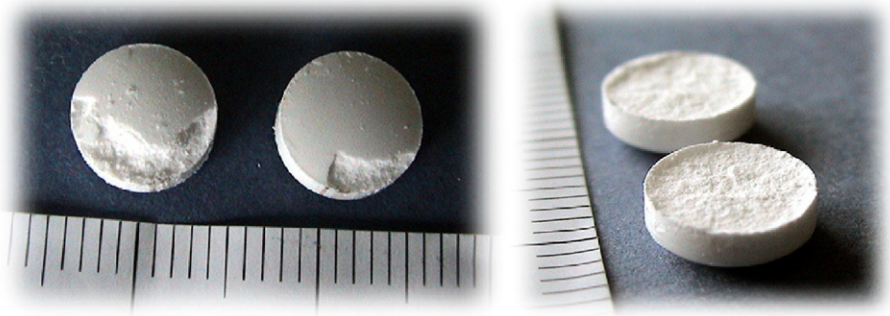

(a) shallow convex tablets (b) standard convextablets

Fig. 15. Photographs of convex lactose tablets.

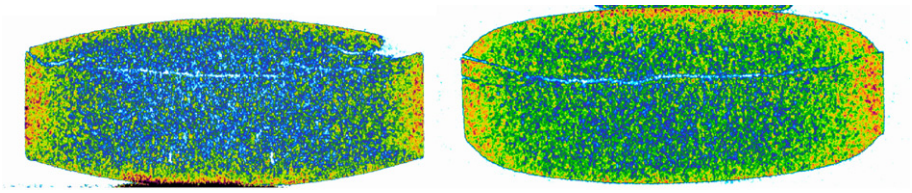

(a) shallow convex tablet (b) standard convex tablet

Fig. 16. X-ray computed micro-tomographic images of convex lactose tablets.

Fig. 16 shows XMT images of the vertical cross-sections of a shallow convex tablet (Fig. 16a) and a standard convex tablet in which no failure is visible from its appearance (Fig. 16b). Figs. 15 and 16 clearly show that capping and cracks were developed along a surface that is less oblique than those observed for flat-faced tablets (Fig. 4). In addition, we have noticed during the experiments that capping takes place when the top punch is withdrawing but the bottom one is still stationary, *i.e.* the decompression phase. This also further confirms that the shear band formed during decompression is one of the primary factors that are responsible for the occurrence of capping as proposed in Ref. [1].

5. Discussion

Numerical and experimental results for the compaction of flat-faced and convex tablets shown in Fig. 4, 14–16 demonstrate that capping and cracking are due to the formation of an intensive shear band during the decompression phase. Therefore, examining if there is an intensive shear band developed during decompression will provide crucial information about whether capping or cracking will occur, and what the possible failure patterns will be during the tabletting process. The results shown in Figs. 6–14 clearly show that there are intensive shear band for all cases considered here. This implies that the various approaches attempted in this study to alleviate the propensity for tablet to cap (including changing the die-wall friction, compaction speed, tablet thickness, compaction profile and punch curvature) will not necessarily be effective.

The patterns of shear band formation during the decompression stage appear to depend primarily on the tablet shape, not on the processing conditions and the materials considered (see, also, Ref. [32]). However, when a different material is used, two important factors have to be taken into consideration: (i) changes in mechanical properties of the bulk materials, such as the properties that are used in FEM analysis, and (ii) changes in inter-particle cohesive bonding strength, which is dominant in determining if the powder can form a cohesive compact. The changes in mechanical properties of bulk materials will not necessarily avoid the formation of a shear band during decompression, as discussed in Ref. [32], and hence similar failure patterns can still be produced. However, changes in particle interfacial properties will make it possible to avoid the occurrence of capping and/or cracking because these phenomena will not occur once the inter-particle cohesive strength is high enough to withstand the breaking forces [7,8], even though a similar shear band pattern is predicted from FE analysis. Although better numerical predictions of the occurrence of capping can be achieved by implementing some failure criteria and by considering the inter-particle cohesive strength, this is not straightforward to do and further investigations are currently in progress. Nevertheless, particle interfacial properties can be indicated to some extent by the bulk tensile strength of the powder. It is known that lactose generally has a very low tensile strength comparing to other common pharmaceutical excipients, and a blend with higher tensile strength can be achieved by mixing it with other excipients of high tensile strength [33]. Therefore, a combined analysis of mechanical behaviour of powders during compaction and mechanical strength of tablets could be beneficial for tablet production.

6. Conclusion

Following on from our recent study [1], which revealed that cone capping occurs as a result of the formation of shear bands during decompression, further systematic studies have been performed to explore possible approaches to avoid the occurrence of capping. These included using lubricants to reduce the die-wall friction, employing different tooling kinematics (changing both compaction speed and compression profiles), increasing the minimum thickness (or reducing the maximum compression pressure) and using punches with curved surfaces to make convex tablets. By using finite element analysis, it has been shown that none of these methods can necessarily avoid the development of intensive shear bands during decompression, implying that it is still possible for capping to be induced. In addition, physical experiments using a compaction simulator have been carried out, in particular for making convex tablets with different surface curvatures. The tablets produced were examined using XMT, and the experiments confirmed that capping and cracking were induced even in convex tablets, as indicated by our numerical analysis. Furthermore, the failure patterns were found to be in very good agreement with those predicted from the finite element simulations. The combination of experimental and numerical analyses has demonstrated that: (i) capping appears to take place during the decompression (unloading) phase, and (ii) the intensive shear band developed during decompression is one of the factors that are responsible for the occurrence of capping.

Acknowledgement

The authors wish to acknowledge Pfizer Global Research and Development for funding this work.

References

[1] C.Y. Wu, O. Ruddy, A.C. Bentham, B.C. Hancock, S.M. Best, J.A. Elliott, Modelling the mechanical behaviour of pharmaceutical powders during compaction, Powder Technology 152 (2005) 107–117.

[2] C.Y. Wu, A.C.F. Cocks, Flow behaviours of powders during die filling, Powder Metallurgy 47 (2004) 127–136.

[3] C.Y. Wu, L. Dihoru, A.C.F. Cocks, The flow of powder into simple and stepped dies, Powder Technology 134 (2003) 24–39.

[4] C.Y. Wu, A.C.F. Cocks, O.T. Gillia, Die filling and powder transfer, International Journal of Powder Metallurgy 39 (2003) 51–64.

[5] G. Alderborn, C. Nystrom, Pharmaceutical Powder Compaction Technology, Marcel Dekker, Inc., New York, 1996.

[6] O. Coube, A.C.F. Cocks, C.Y. Wu, Experimental and numerical study of die filling, powder transfer and die compaction, Powder Metallurgy 48 (2005) 68–76.

[7] S.K. Dwivedi, R.J. Oates, A.G. Mitchell, Estimation of elastic recovery, work of decompression and Youngs modulus using a rotary tablet press, Journal of Pharmacy and Pharmacology 44 (1992) 459–466.

[8] K. Sugimori, S. Mori, Y. Kawashima, Characterisation of die wall pressure to predict capping of flat- or convex-faced drug tablets of various sizes, Powder Technology 58 (1989) 259–264.

[9] L. Casahoursat, G. Lemagnen, D. Larrouture, The use of stress–relaxation trials to characterise tablet capping, Drug Development and Industrial Pharmacy 14 (1988) 2179–2199.

[10] T. Tanino, Y. Aoki, Y. Furuya, K. Sato, T. Takeda, T. Mizuta, Occurrence of capping due to insufficient air escape during tablet compression and a method to prevent it, Chemical and Pharmaceutical Bulletin 43 (1995) 1772–1779.

[11] I.C. Sinka, J.C. Cunningham, A. Zavaliangos, The effect of wall friction in the compaction of pharmaceutical tablets with curved faces: a validation study of the Drucker–Prager cap model, Powder Technology 133 (2003) 33–43.

[12] R.M. Nedderman, Statics and Kinematics of Granular Materials, Cambridge University Press, New York, 1992.

[13] X. Fu, N. Dutt, A.C. Bentharn, B.C. Hancock, R.E. Cameron, J.A. Elliott, Investigation of particle packing and compaction in model pharmaceutical powders using X-ray microtomography and discrete element method, Powder Technology 167 (2006) 134–140.

[14] S.R. Stock, X-ray microtomography of materials, International Materials Reviews 44 (1999) 141–164.

[15] E. Maire, J.-Y. Buffière, L. Salvo, J.J. Blandin, W. Ludwig, J.M. Letang, On the application of X-ray microtomography in the field of materials science, Advanced Engineering Materials 38 (2001) 539–546.

[16] T. Ohtani, Y. Nakashima, H. Muraoka, Three-dimensional miarolitic cavity distribution in the Kakkonda granite from borehole WD-1a using X-ray computerized tomography, Engineering Geology 56 (2000) 1–9.

[17] J.-Y. Buffière, S. Savelli, P.H. Jouneau, E. Maire, R. Fougères, Experimental study of porosity and its relation to fatigue mechanisms of model Al–Si7–Mg0.3 cast Al alloys, Materials Science & Engineering. A, Structural Materials: Properties, Microstructure and Processing A316 (2001) 115–126.

[18] M. Preuss, P.J. Withers, E. Maire, J.-Y. Buffière, SiC single fibre full-fragmentation during straining in a Ti–6Al–4V matrix studied by synchrotron X-rays, Acta Materialia 50 (2002) 3175–3190.

[19] T.J. Marrow, H. Çetinel, M. Al-Zalmah, S. MacDonald, P.J. Withers, J. Walton, Fatigue crack nuclei in austempered ductile cast iron, Fatigue & Fracture of Engineering Materials & Structures 25 (2002) 635–648.

[20] L. Babout, W. Ludwig, E. Maire, J.Y. Buffière, Damage assessment in metallic structural materials using high resolution synchrotron X-ray tomography, Nuclear Instruments and Methods in Physics Research. Section B, Beam Interactions with Materials and Atoms 200 (2003) 303–307.

[21] L.B. Wang, J.D. Frost, G.Z. Voyiadjis, T.P. Harman, Quantification of damage parameters using X-ray tomography images, Mechanics of Materials 35 (2003) 777–790.

[22] I. Aydin, B.J. Briscoe, K.Y. sanlitürk, The internal form of compacted ceramic components: a comparison of a finite element modelling with experiment, Powder Technology 89 (1996) 239–254.

[23] I. Aydin, B.J. Briscoe, N. Ozkan, Modelling of powder compaction: a review, MRS Bulletin (1997) 45–51.

[24] PM MODNET, Research Group, Numerical simulation of powder compaction for two multilevel ferrrous parts, including powder characterisation and experimental validation, Powder Metallurgy 45 (2002) 335–343.

[25] PM MODNET, Computer Modelling Group, Comparison of computer models representing powder compaction process, Powder Metallurgy 42 (1999) 301–311.

[26] O. Coube, H. Riedel, Numerical simulation of metal powder die compaction with special consideration of cracking, Powder Metallurgy 43 (2000) 123–131.

[27] A. Zavaliangos, Constitutive models for the simulation of P/M process, The 2002 Internation Conference on Process Modelling in Powder Metallugy and Particulate Materials, Princeton, NJ, MPIF, 2002.

[28] A. Michrafy, D. Ringenbacher, P. Techoreloff, Modelling the compaction behaviour of powders: application to pharmaceutical powders, Powder Technology 127 (2002) 257–266.

[29] ABAQUS Theory Manual, Version. 6.4, HKS Inc, 2004.

[30] N. Zahlan, D.T. Knight, A. Backhouse, G.A. Leiper, Modelling powder compaction and pressure cycling, Powder Technology 114 (2001) 112–117.

[31] C.Y. Wu, J.A. Elliott, A.C. Bentham, S.M. Best, B.C. Hancock, W. Bonfield, A numerical study on the mechanical behaviour of pharmaceutical powders, Proc. Int. conf. on Pharmaceutics, Biopharmaceutics and Pharmaceutical Technology, 15th–18th March, Nuremberg, Germany, 2004, pp. 17–18.

[32] C.Y. Wu, B.C. Hancock, J.A. Elliott, S.M. Best, A.C. Bentham, Bonfield, Finite element analysis of capping mechanisms during pharmaceutical powder compaction, Advances in Powder Metallurgy and Particulate Materials 1 (2005) 62–73.

[33] C.Y. Wu, S.M. Best, A.C. Bentham, B.C. Hancock, W. Bonfield, A simple predictive model for the tensile strength of binary tablets, European Journal of Pharmaceutical Sciences 25 (2005) 331–336.